44th Turbomachinery
31st Pump SYMPOSIA
GEORGE R. BROWN CONVENTION CENTER
HOUSTON, TX | SEPT. 14 - 17, 2015

Axial Thrust in High Pressure Centrifugal Compressors: Description of a Calculation Model Validated by Experimental Data from Full Load Test

Leonardo Baldassarre
Engineering Executive for Compressors and Auxiliary Systems
General Electric Oil & Gas Company
Florence, Italy

Andrea Bernocchi
Senior Engineering Manager for Centrifugal Compressors
General Electric Oil & Gas Company
Florence, Italy

Emanuele Rizzo
Senior Design Engineer for Centrifugal Compressors
General Electric Oil & Gas
Florence, Italy

Michele Fontana
Engineering Manager for Centrifugal Compressors
General Electric Oil & Gas
Florence, Italy

Francesco Maiuolo
Lead Design Engineer for Heat Transfer & Secondary Flows
General Electric Oil & Gas
Florence, Italy

Leonardo Baldassarre is currently Engineering Executive Manager for Compressors and Auxiliary Systems with GE Oil & Gas, in Florence, Italy. He is responsible for requisition and standardization activities and for the design of new products for compressors, turboexpanders and auxiliary systems.
Dr. Baldassarre began his career with GE in 1997. He worked as Design Engineer, R&D Team Leader, Product Leader for centrifugal and axial compressors and Requisition Manager for centrifugal compressors.
Dr. Baldassarre received a B.S. degree (Mechanical Engineering, 1993) and Ph.D. degree (Mechanical Engineering / Turbomachinery Fluid Dynamics, 1998) from the University of Florence. He authored or coauthored 20+ technical papers, mostly in the area of fluid dynamic design, rotating stall and rotordynamics. He presently holds five patents.

Andrea Bernocchi is an engineering manager at GE Oil&Gas. He joined GE in 1996 as Centrifugal Compressor Design Engineer after an experience in plastic machinery industry. He has 18 years of experience in design development, production and operation of centrifugal compressor. He covered the role of LNG compressor design manager for 6 years with responsibility in design of LNG compressors, testing and supporting plant startup. He's currently leading the requisition team for centrifugal and axial compressor design.
Mr. Bernocchi received a B.S. degree in Mechanical Engineering from University of Florence in 1994. He holds 4 patents in compressor field.

Michele Fontana is currently Engineering Manager for Centrifugal Compressor Upstream, Pipeline and Integrally Geared Applications at GE Oil&Gas, in Florence, Italy. He supervises the calculation activities related to centrifugal compressor design and testing, and has specialized in the areas of rotordynamic design and vibration data analysis.
Mr. Fontana graduated in Mechanical Engineering at University of Genova in 2001. He joined GE in 2004 as Centrifugal Compressor Design Engineer, after an experience as Noise and Vibration Specialist in the automotive sector.
He authored or co-authored eight technical papers about rotordynamic analysis and vibration monitoring, and holds two patents in this same field.

Emanuele Rizzo is currently Senior Design Engineer in New Product Introduction for Centrifugal Compressors with GE Oil&Gas, Florence, Italy. His current duties are mainly focused on structural design, material selection and new applications of centrifugal compressors.
Dr. Rizzo holds an MSc degree (Aerospace Engineering, 2003) and a Ph.D. degree (Aerospace Engineering, Conceptual Aircraft Design and Structural Design, 2007) from the University of Pisa (Italy). He joined GE Oil&Gas in 2008 as Lead Design Engineer in the centrifugal compressors requisition team, working mainly on high pressure compressors operating in sour environment.
He has authored and coauthored several papers on aircraft design and optimization. He is co-inventor in two patents.

Francesco Maiuolo is currently Lead Design Engineer in the Advanced Technology Organization of GE Oil&Gas, Florence, Italy. Dr. Maiuolo received his MSc degree in Energy Engineering in 2009 and the Ph.D. degree (Energy Engineering Department, 2013) from the University of Florence (Italy). He joined GE Oil&Gas in early 2013 in the Aero-thermal design team, mainly focusing on heat transfer, secondary flows and sealing systems of rotating machinery as centrifugal compressors and gas turbines.
He authored or co-authored ten technical papers on heat transfer and secondary flows studies.

ABSTRACT

The residual axial thrust acting on the rotor of a centrifugal compressor is the result of the non-uniform pressure distribution on the surfaces in contact with the process gas, plus the differential pressure acting on the faces of the balance piston(s) and the contribution due to the momentum variation of the process gas. During the design phase the axial load shall be verified to remain safely lower than the thrust bearing capacity, under all possible operating conditions; this requires a high degree of accuracy in the calculation model used to evaluate each thrust component. Errors in this calculation may lead to high bearing pad temperature during operation, to early wearing of the pad surfaces and ultimately to the damage or failure of the thrust bearing (Moll and Postill, 2011), thus jeopardizing the integrity of the whole compressor.

The main difficulty of axial thrust calculation lies in the correct prediction of the static pressure distribution over the external surface of the impeller hub and shroud. This distribution depends on a large set of parameters, including rotor geometry, operating conditions, properties of the process gas, leakages flows across the rotor-stator seals. A detailed fluid-dynamic model of the gas in the cavities between impeller and diaphragm was developed and applied first to stage model tests and then to high-pressure centrifugal compressors, and its predictability was assessed by direct comparison with experimental data. The compressors were tested in full load conditions, with thrust bearing pads equipped with load cells, and the thrust values were recorded for several points across the operating envelope.

INTRODUCTION

The accurate prediction of axial thrust is a key factor for the correct design of a centrifugal compressor. The correct selection of the thrust bearing and the sizing of the balance drum(s) are assessed by evaluating the residual axial thrust across the operating envelope and the consequent bearing pad load and temperature.

Standard requirements for the selection of the thrust bearing impose limits on the maximum allowable load and temperature (API617, 2014). In order to comply with these requirements, OEMs have developed internal design criteria and defined safety margins based on their own experience.

Axial thrust prediction is directly related to the calculation of the gas pressure acting on the surfaces of the rotor, that is particularly challenging for the external surfaces of the impellers. Here the pressure distribution is heavily affected by aerodynamic effects related to the gas flowing in the rotor-stator cavities, that are function of a large set of geometric and thermodynamic data, as summarized in the next section. A software tool was developed to solve this physical model and to calculate the resulting axial force acting on the rotor.

The present work provides a description of the tool and of the model adopted to simulate the physical system and governing laws. The validation of the tool is then addressed, by comparing its predictions to the experimental results collected on model tests of single stages and on full load tests of complete centrifugal compressors. The experimental data are further analyzed, providing insights of other features that can be identified and explained basing on the knowledge of the physical model and its governing laws.

Conclusions derived from this study provide some recommendations on centrifugal compressor axial thrust evaluation and on the physical model .

THRUST CALCULATION

During operation the rotor of a centrifugal compressor is subject to an axial thrust T resulting from the sum of several components:

- T_m due to variation of gas momentum
- T_a due to differential pressure across the impellers
- T_b due to differential pressure across the balance piston
- T_c due to coupling pre-stretch

$$T = T_m + T_a + T_b + T_c \quad (1)$$

The present analysis is focused on the evaluation of aerodynamic effects and therefore does not address the coupling pre-stretch contribution, which is generally compensated by the thermal deformation of the shaft and has very limited impact during normal compressor operation. The other effects are described in detail below.

Axial thrust due to momentum variation

An axial force is generated on the rotor as a result of the momentum variation of the gas flow, and specifically by the difference of gas axial speed between impeller inlet and outlet (see Figure 1):

$$T_m = \dot{m} v_{ax\,OUT} - \dot{m} v_{ax\,IN} \quad (2)$$

with axial thrust considered positive in the direction of impeller suction. In case of radial gas exit the term $v_{ax\,OUT}$ is equal to zero and Equation (2) becomes:

$$T_m = -\dot{m}_{IN} v_{ax\,IN} \quad (3)$$

This force is directed towards compressor discharge.

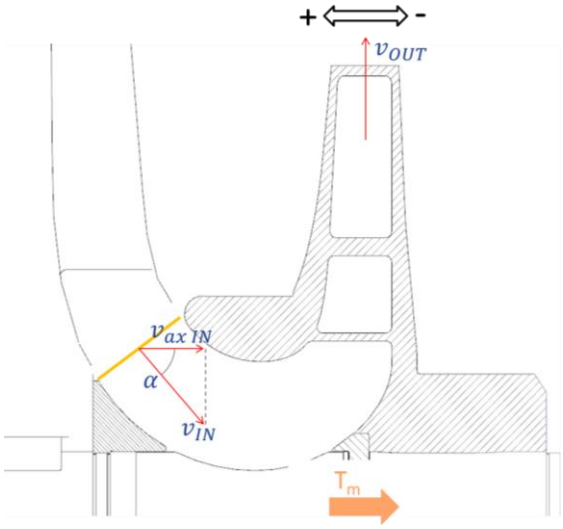

Figure 1. Variation of gas momentum

The control volume for the momentum balance shall include the part of the rotor in front of the impeller (in Figure 1, the shaft portion and the triangular sleeve section on the left side). This leads to a reduction of T_m, as a function of the α angle as shown in Figure 2, since:

$$v_{ax\,IN} = v_{IN} \cos \alpha \quad (4)$$

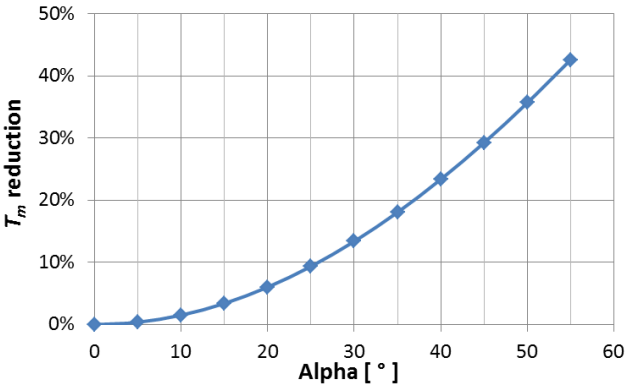

Figure 2. Reduction of thrust component T_m due to stage inlet geometry

Axial thrust on impeller due to gas pressure

Figure 3 shows the pressure distribution over the rotor portion corresponding to one compressor stage. For the sake of simplicity the labyrinth seal is considered plain (same inner diameter for all teeth): in case the impeller eye is stepped, an additional contribution acting on the impeller eye shall be accounted for.

The axial force due to gas pressure can be calculated by integrating the axial component of the pressure distribution over the rotor surfaces. With the same sign convention of Figure 1:

$$T_a = \int_{A_H} p\, dA - \int_{A_S} p\, dA - \int_{A_{IN}} p\, dA \quad (5)$$

where A_{IN}, A_H, A_S are the inlet, hub and shroud areas respectively, and are defined below:

$$A_H = \frac{\pi}{4}\left(D_{tip}^2 - D_{foot}^2\right) \quad (6)$$

$$A_S = \frac{\pi}{4}\left(D_{tip}^2 - D_{eye}^2\right) \quad (7)$$

$$A_{IN} = \frac{\pi}{4}\left(D_{eye}^2 - D_{foot}^2\right) \quad (8)$$

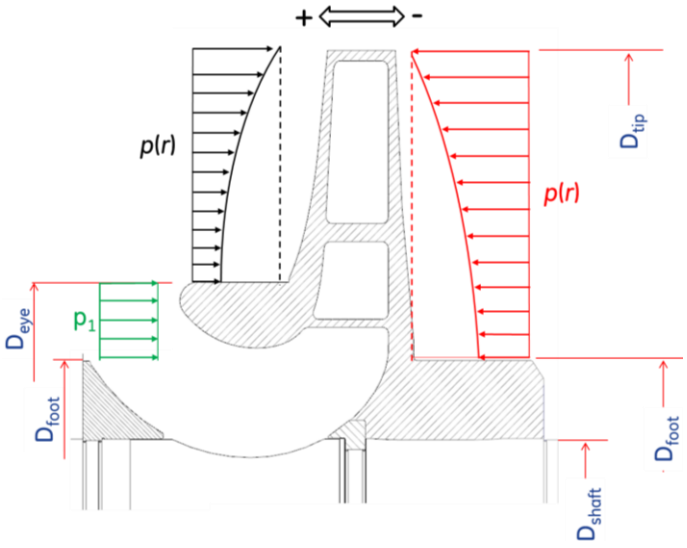

Figure 3. Pressure distribution on a compressor stage.

The pressure can be assumed constant over the impeller inlet area A_{IN} and therefore the last integral of Equation (5) is simply equal to $p_1 A_{IN}$, while this assumption is not valid for A_H and A_S. As reported in literature (Owen and Rogers, 1989), the gas pressure on a rotating disk enclosed in a cavity varies in the radial direction with a trend that is strongly related to the core rotating speed of the gas within the cavity, that in turn is a function of the gas flow rate in the radial direction. For the addressed case of centrifugal compressor impellers, this flow rate is the leakage across impeller labyrinth seals: therefore the pressure distribution is strongly affected by seal clearances and by compressor operating conditions, determining the pressure ratio across the seal (Kurz et al., 2011).

In the present work the term *primary effect* (T_I) is used to define the axial thrust calculated considering a constant pressure distribution in the impeller-diaphragm cavities:

$$T_I = p_2 A_H - p_1 A_{IN} - p_2 A_S \quad (9)$$

with p_1 and p_2 defined as the static pressure at impeller sinlet and outlet. We define *secondary effect* (T_{II}) the difference between the exact estimation T_a of this thrust as per Equation 5 and the constant-pressure approximation represented by T_I:

$$T_{II} = T_a - T_I \quad (10)$$

The denomination is justified mainly because the constant pressure profile is modified by secondary flows in the cavity.

The radial pressure distribution along the hub and shroud cavities is governed by the following equations:

$$\begin{cases} \frac{1}{\rho}\frac{dp}{dr} = \omega^2 k^2 r \\ p(r_2) = p_2 \end{cases} \quad (11)$$

where k is the core rotation coefficient, that relates the angular velocity of the flow in the cavity to the angular velocity of the impeller. The cavity inlet pressure is approximately equal to the pressure p_2 at the impeller exit.

Equation 11 defines a parabolic trend of the pressure along the cavity radius, whose shape is determined by the value of k factor. The authors developed a tool for calculating the pressure distribution of the gas inside the cavity, whose radial section is divided in a series of control volume elements. The balance of the angular momentum of the gas is performed dividing the cavity in several control volumes and solving the equation for each element:

$$M_{R,i} - M_{S,i} = \dot{m}\,(\omega_2 r_2^2 - \omega_1 r_1^2) \quad (12)$$

where subscripts 1 and 2 are related to control volume inlet and outlet. M_R and M_S are the torque terms for the rotating and stationary surfaces respectively, calculated as:

$$M_{R,i} = \left(\frac{\rho C_{f,R}}{2}\right)_i \omega^2 (1-k)^2 \int_{AR,i} r^3 dA \quad (13)$$

$$M_{S,i} = \left(\frac{\rho C_{f,S}}{2}\right)_i \omega^2 \int_{AS,i} r^3 dA \quad (14)$$

where $C_{f,R}$ and $C_{f,S}$ are the momentum coefficients for rotor and stator respectively. They are dependent on the local rotational Reynolds number, and are evaluated by means of experimental correlations as described in detail in (Da Soghe et al., 2009). The correct evaluation of these coefficients, and therefore of the core rotation of the gas in the cavities, is necessary to predict with accuracy the residual axial thrust on the rotor, particularly for high pressure applications.

Net axial thrust

The net axial force acting on the thrust bearing is given by Equation (1), that in view of the above considerations can be rewritten as:

$$T = T_I + T_{II} + T_b + T_m \quad (15)$$

where the thrust component T_b can be calculated assuming constant pressure distribution on the balance drum faces (secondary effects are generally negligible on this component).

THRUST PREDICTION AND VALIDATION THROUGH EXPERIMENTAL DATA

The software tool used for axial thrust prediction is based on the physical model described in the previous section. It is composed of a 1D flow network solver that is able to process networks composed by cavities, seals and combinations of them. The main results of the calculation are the pressure distributions inside the cavities and the flow rate of the gas leakages though the seals. These results allow to evaluate the total thrust acting on the rotating surfaces.

To validate the tool, the calculated pressure distribution inside the cavity was compared with experimental data available from stage model tests and from a dedicated centrifugal compressor test vehicle (typical rotational Reynolds numbers around 10^6). Another comparison was carried out with experimental data from the full load test of two high pressure compressors equipped with load cells on thrust bearing pads (typical rotational Reynolds numbers around 10^8).

Validation on model test data

Measures on model tests have been carried out for several impellers with different flow coefficient and diameter, varying the values of inlet pressure and rotating speed. Figure 4 shows a typical model test instrumented with static pressure taps.

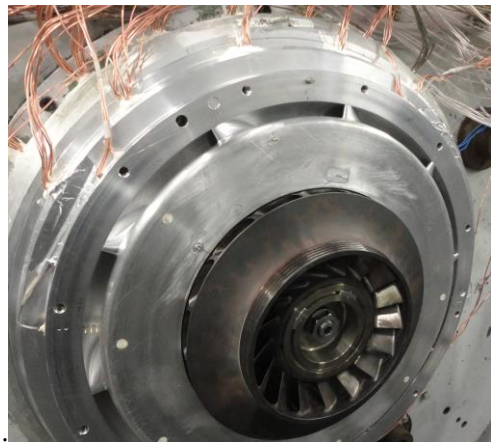

Figure 4. Picture of a stage model test

Comparisons between measurements and calculation results were performed on hub and shroud sides of several centrifugal compressor impellers; two cases are presented in this section. Figure 5 and Figure 6 show the cross sections of the tested impellers and the data comparison on a normalized radius vs. pressure plot. As shown in sketch drawings, both hub and shroud cavities are instrumented with three static pressure taps and two J-type thermocouples to record the gas temperature at cavity inlet and outlet. Static pressures are measured with a differential pressure scanner, characterized of an uncertainty error of 0.1% full scale.

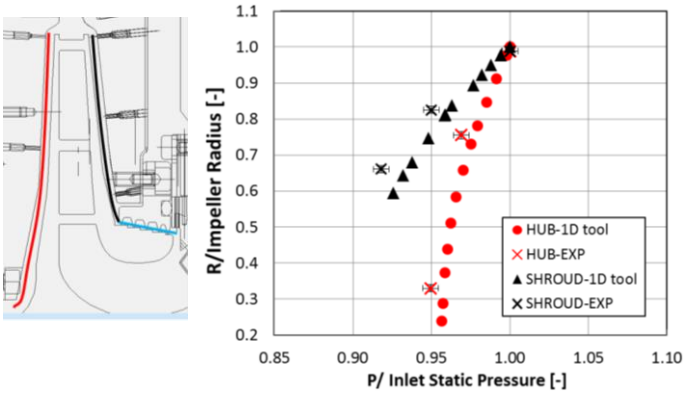

Figure 5. Comparisons between pressure measurements and 1D tool for impeller 1.

In Figure 5 the red marks represent the data on the hub side and thee black ones represent the data on shroud side. A quite good agreement is visible between measurements and 1D tool results along the radius of the cavities. In particular the calculation code correctly estimates the shape of the pressure profile along the cavity, for both hub and shroud sides. However, for some cases not negligible differences have been found due to the uncertainty in the boundary conditions that substantially affect the static pressure gradient:

- Rotation factor of the flow entering in the cavity (*k*). This parameter is estimated with significant uncertainty, and its value has a direct influence on the prediction of the pressure gradient in the cavities.
- Inlet static pressure. In first approximation it is assumed equal to the static pressure at impeller outlet. Actually there are small deviations from this pressure value for both hub and shroud cavity inlet, that may limit the accuracy of the primary thrust calculation.
- Seal clearance: this parameter determines the gas leakage flow rates, that have a significant influence on the pressure distribution in the cavity and therefore on the magnitude of the axial thrust, as discussed in (Bidaut et al., 2009 and 2014).
- Friction coefficient: the estimation of the friction coefficient of rotor and stator surfaces impacts the rotation factor calculation (Gülich, 2003).

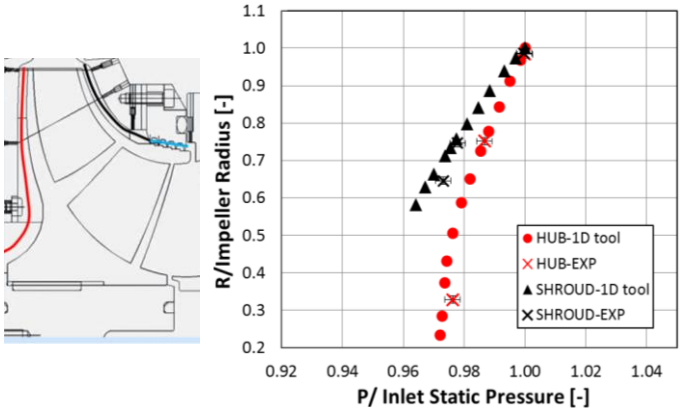

Figure 6. Comparisons between pressure measurements and 1D tool for impeller #2.

The matching between measured and expected data is better for impeller #2 (Figure 6) than for impeller #1 due to the shape of the impeller that leads to a lower variation of the radial pressure inside the cavities.

Validation on centrifugal compressor test vehicle data

The development of a test vehicle of a back-to-back high pressure compressor (Figure 7) provided a good opportunity to validate the 1D tool in high pressure conditions. The compressor is composed of 4 stages in the first phase and 5 stages in the second.

For tool validation, two stages (the 1st and the 6th) have been instrumented with three static pressure taps inside shroud and hub cavities, with the same approach used for model test probe positioning. All the inlet boundary conditions used to run the calculations are taken from test measurements.

The tests were performed with gas molecular weight of 22.4kg/kmol, at 10200rpm running speed and with final discharge pressure of 408 bar.

Figure 8 shows the comparisons between measured and expected pressure values inside the hub and shroud cavities of the 1st stage. It confirms that the calculation tool is able to catch the pressure trend also for high pressure conditions. Residual differences between measures and calculations are mainly due to uncertainties in the boundary conditions imposed to the tool. In particular, as already seen in model test comparisons, the seal clearances have a non-negligible impact to the calculated pressure distribution, leading to a rotation of the curve. A higher clearance means a high mass flow rate across the seal and consequently to a reduced variation of pressure along the radius (Gülich, 2003). Rotation of the curve can be noted also changing the inlet swirl, while an error in the inlet static pressure causes a shift of the curve along the *x* axis. The comparisons were performed considering the clearance measured at compressor assembly, hence in cold and non-rotating conditions.

Figure 7. Compressor Test Vehicle setup.

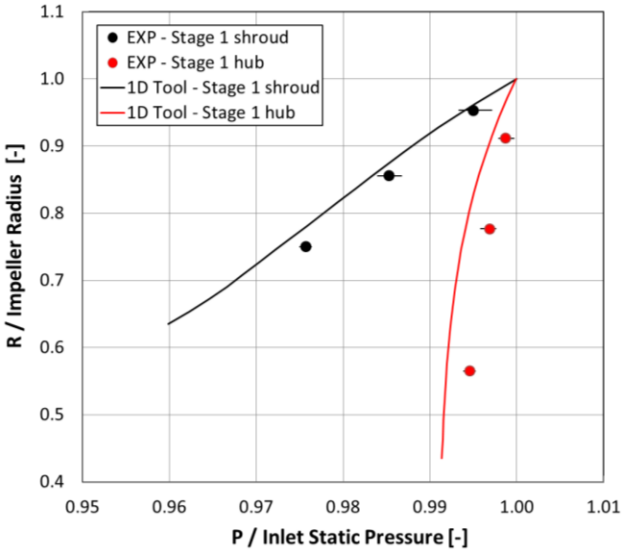

Figure 8. Comparisons between pressure measurements in Test Vehicle and 1D tool, 1st stage.

Results relative to the 6th stage are presented in Figure 9; the comparison confirms good agreement between measured and calculated static pressures for both the hub and shroud cavities.

Axial Thrust Measurements

Two different centrifugal compressors were equipped with load cells on thrust bearing (Figure 10), allowing the direct measure of the residual axial thrust. These compressors were selected among the most representative for this kind of test activity, sharing the following features:

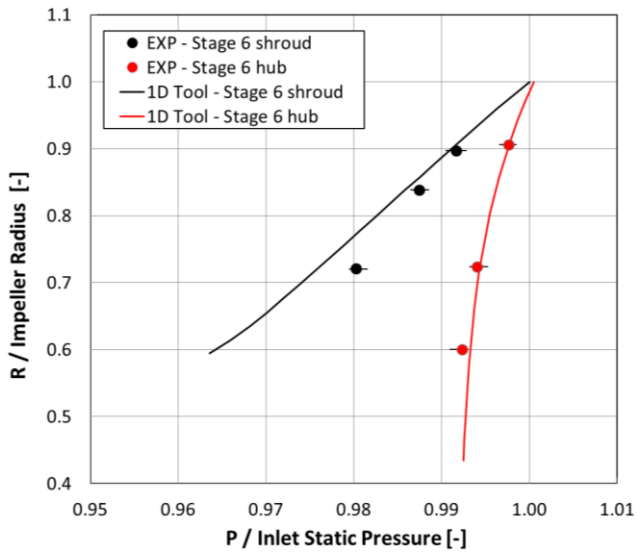

Figure 9. Comparisons between pressure measurements in Test Vehicle and 1D tool, 6th stage.

- Single section, in-line impeller arrangement, simplifying the physical model of the system.
- High gas pressure and density, corresponding to high secondary effects, that represent the most challenging element for axial thrust prediction.
- Presence of a full load test or ASME PTC-10 Type 1 test, allowing the direct measure of the thrust in conditions as close as possible to the design ones

Figure 10. Picture of a thrust bearing pad with load cell.

A summary of the main compressor parameters is presented in Tables 1 and 2, together with relevant thrust bearing data. Load cells were installed on both sides of the thrust bearings.

During the string test the inlet conditions (pressure, MW, temperature) remained almost constant, only speed and flow were varied during the test (Figure 11). Measures are compared with calculation results at Figures 12-13.

Unit	No. stages	Suction pressure [bar-a]	Discharge pressure [bar-a]	Speed [rpm]	Avg. Gas Density [kg/m^3]
#1	5	83	234	6500-9770	100
#2	5	89	205	6000-9000	95

Table 1. Main operating conditions for considered compressors

Unit	Thrust Bearing type	N. of Pads	N. of load cells
#1	Direct Lube	8	4+2
#2	Flooded	6	3+2

Table 2. Data of thrust bearings and load cells. Load cell number refers to active+inactive side.

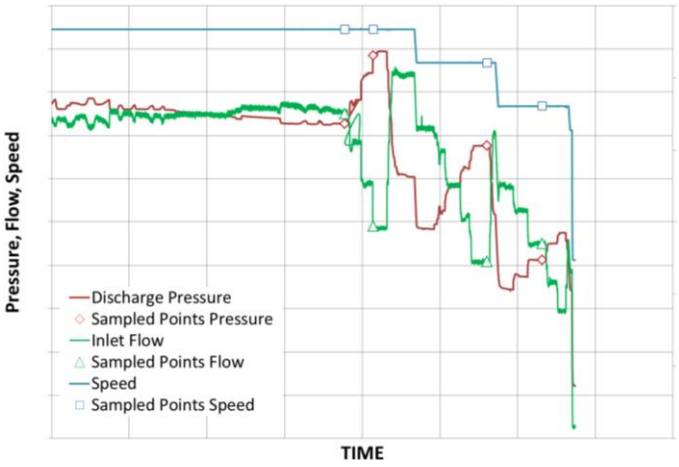

Figure 11. Trend of speed, flow rate and axial thrust in a part of the test of Unit #1.

Data from the string test of Unit #1 were analyzed at two different speed values, 8400 and 9300 rpm, as reported in Figure 12. Four measurement points are available for each speed, at flow rate ranging between 150 kg/s and 200 kg/s. The solid lines correspond to the predicted thrust curves, calculated considering all the contributions of Equation (1). The matching between predicted curves and test data is fairly good, in particular at design operating condition. The largest discrepancies between measurements and calculations are around the 20% , and they have been found at the lowest mass flow rate. On calculation side these differences can be ascribed to the assumptions done for the boundary conditions that cannot be measured directly (i.e. inlet swirl, seal clearances in operating conditions etc.). On experimental side the error bars in the diagram show the dispersion associated to the values (measures were repeated at different circumferential positions and then averaged); the error range of the probes and measurement chain is comparatively negligible.

For Unit #2, measurements were performed in string test at 9100rpm (Figure 13). The solid line corresponding to the calculated global residual thrust is in quite good agreement with measured data, in particular with regard to the trends. Also in this case some non-negligible differences can be noted due to the uncertainties discussed above.

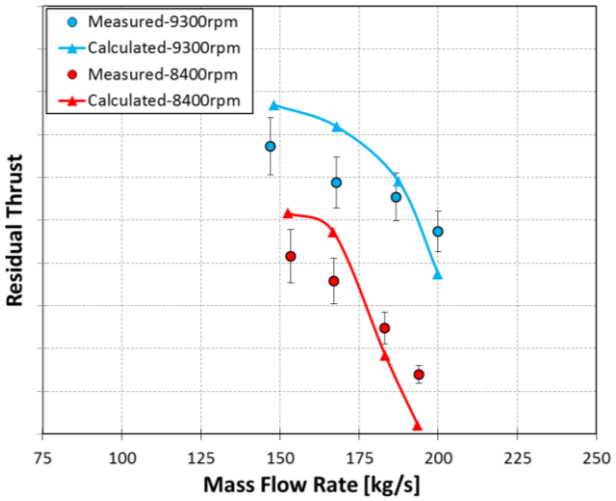

Figure 12. Measured and predicted axial thrust for Unit #1, at two running speeds.

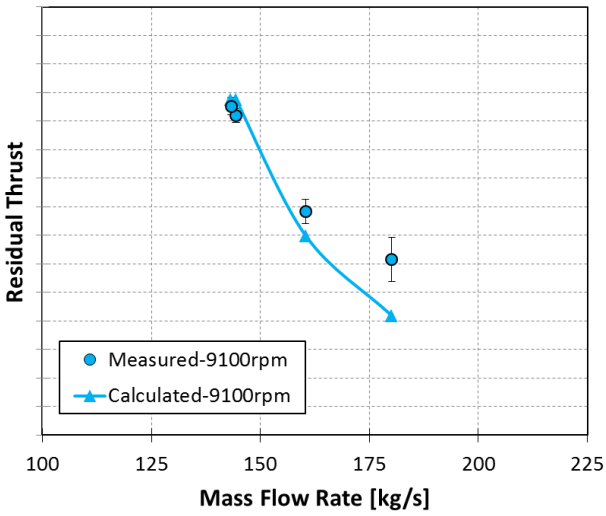

Figure 13. Measured and predicted axial thrust for Unit #2.

Axial displacement vs. thrust bearing load

The experimental data gathered during the tests of the two compressors equipped with load cells have provided material for additional considerations and analyses of compressor thrust.

In Figure 14 the axial load measured on the two sides of the thrust bearing is plotted versus the displacement measured by axial probes, for the full load test of Unit #1. All thrust and displacement values are averaged over two probes' measurements. The two curves are roughly symmetric, as expected for a double-acting thrust bearing with similar geometry on the two sides. It is interesting to note that when the bearing is in neutral position (points closest to the vertical axis) and therefore the residual thrust is approximately zero, the load

cells of both sides detect a positive load. This load is induced by the viscous forces of the oil that is revolving in the bearing, and generates a hydrodynamic load on the bearing pads. This same behavior can be observed in detail in Figure 15, showing the axial load on both sides of the bearing during compressor operation at constant speed (6540rpm) and variable inlet flow rate. At high flow the load acting on the NDE side is zero, then when the flow is reduced the load increases on NDE and decreases on DE side, but remains positive on both sides.

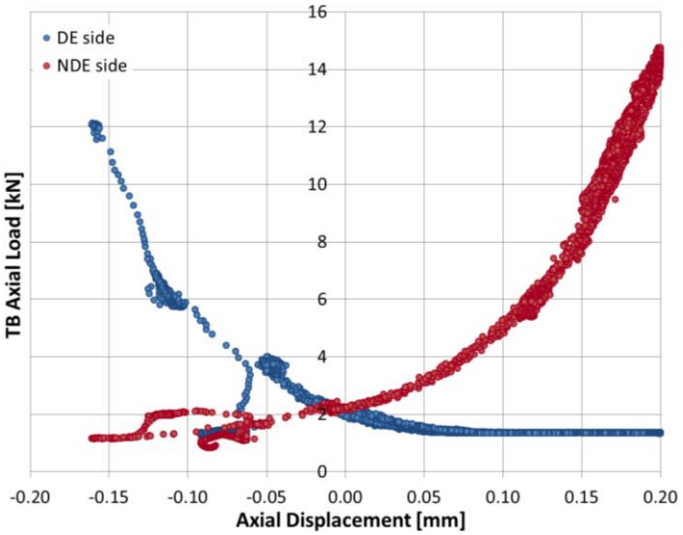

Figure 14. Correlation between axial displacement and bearing load (Unit #1).

The slope of the curve in Figure 14 is a ratio between a force (load acting on the bearing) and a displacement in the direction of the force, therefore it represents a stiffness. It is the axial stiffness of thrust bearing, and as expected it increases for higher displacements from the bearing centerline, due to the nonlinear relation between oil film width and pressure. In particular there is a good accordance of the experimental data set with the algebraic relation between axial displacement and reacting force F_R that is generally assumed for fluid film bearings (Halling, 1978):

$$F_R = \frac{a}{C^2} \tag{16}$$

where a is a scalar factor (constant) and C is the axial clearance (distance between the thrust collar and the thrust bearing pad surface).

Since the axial displacement x is commonly measured from a centered bearing position (x=0 when the thrust collar is at equal distance from the two sides of the thrust bearing), the clearance C is equal to the difference between half of the bearing end play d and the displacement x:

$$C = \frac{d}{2} \pm x \tag{17}$$

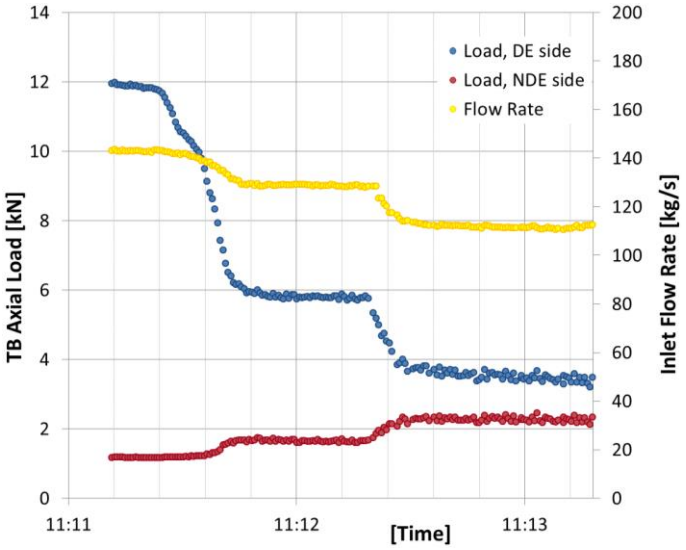

Figure 15. Axial load variation on the two sides of the thrust bearing, at constant speed and varying flow rate (Unit #1).

Considering just one side of the bearing, for example the NDE side, Equation 16 becomes:

$$F_R = \frac{a}{\left(\frac{d}{2} - x\right)^2} \tag{18}$$

In Figure 16 this curve is plotted (with d = 0.6mm) over the experimental curve for the NDE side of Unit #1. The good agreement between experimental data and analytical curve suggest that, in the common case where direct measures of thrust bearing load are not available, variations of axial displacement can be used for a rough estimation of the axial load acting on the bearing.

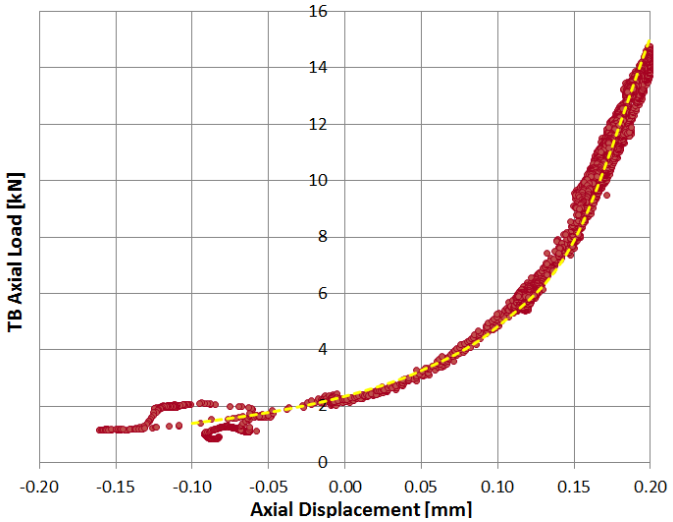

Figure 16. Axial load vs. displacement: experimental data and approximating curve ($1/C^2$).

Other correlations, for example with the thrust bearing pad temperature (see Figure 17) can be used, but they are defined by more complicated models, are affected by higher dispersion of the measurements (different values obtained by probes on different pads) and are heavily influenced by external factor (lube oil temperature, lube oil flow rate, ...) to which the axial displacement is almost insensitive. It shall be noted that the correlation between axial load and displacement is reliable when monitoring variations within a limited time span, while during long term compressor operation it may be biased by the wearing of the bearing pad surface, that leads to an increase of the end play *d*.

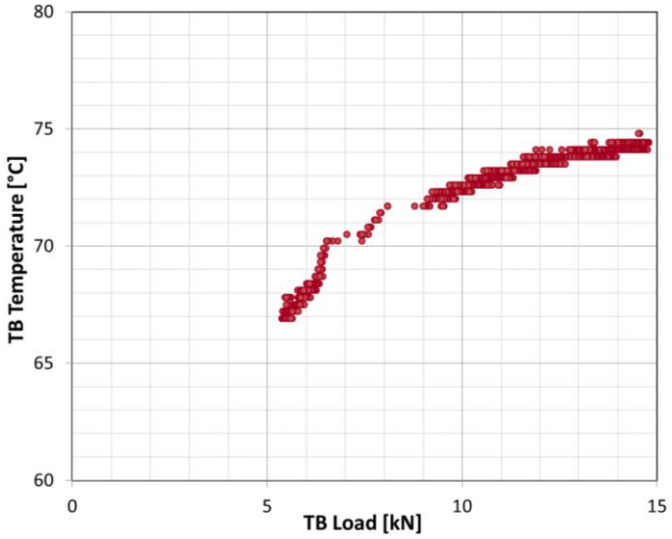

Figure 17. Plot of bearing pad temperature vs. load (at constant speed).

CONCLUSIONS

The main parameters that compose the axial thrust acting on centrifugal compressor rotors were highlighted. The calculation of each parameter and the related uncertainty is a key factor to correctly predict the residual thrust and consequently for thrust bearing selection and balance drum sizing. One of the most challenging and critical aspect is the correct prediction of the static pressure distribution along the impeller hub and shroud cavities, in particular for narrow cavities and large pressure gradients that are typical of high-pressure centrifugal compressors. A 1D software tool was developed to calculate the radial pressure gradient developing along impeller surfaces, and consequently the total axial thrust acting on the rotor.

The tool was validated by comparing calculated pressures with experimental data measured at low pressure (single stage model tests) and at high pressure (full compressor test vehicle). In both cases the comparison highlighted a good agreement between measurements and calculation. The correct prediction of pressure distribution is the starting point for an accurate modeling and evaluation of the so-called "secondary effects", that have a great impact on the total axial thrust of high-pressure compressors. The influence of parameters such as seal clearances and inlet cavity swirl, that cannot be measured directly during compressor operation, puts some limits to the accuracy of comparisons with experimental data.

Moving from the analysis of pressure gradients to the prediction of the global axial thrust, calculation results were compared with data recorded on two high-pressure centrifugal compressors, tested at full load and equipped with load cells on thrust bearings. The results confirmed the good predictability of the software tool also in integral terms.

Besides software validation, the analysis of measured and calculated data sets provided an insight on some phenomena related to axial thrust and on correlations between axial thrust, shaft displacements and bearing pad temperature.

NOMENCLATURE

Acronyms

1D	One-dimensional
DE	Driven End
MW	Molecular weight
NDE	Non Driven End

Symbols

a	*Costant*	[-]
A	Area	[m^2]
C	Bearing clearance	[m]
d	Thrust bearing end play	[m]
D	Diameter	[m]
F	Force	[N]
k	Core rotational factor	[-]
$\dot{m}$	Mass flow	[kg/s]
M	Torque	[N·m]
p	Pressure	[Pa]
r	Radius	[m]
T	Axial Thrust	[N]
v	Velocity	[m/s]
x	Axial displacement	[m]
α	Angle	[deg]
ε	Bearing eccentricity	[-]
μ	Dynamic viscosity	[Pa·s]
ρ	Density	[kg/m^3]
ω	Angular speed of the rotor	[rad/s]

Nondimensional groups

C_f	Momentum coefficient	$\frac{2M}{\rho\omega^2(r_{out}^5 - r_{in}^5)}$
Re	Rotational Reynolds number	$\frac{r^2\omega\,\rho}{\mu}$

REFERENCES

API 617, 2014, "Axial and Centrifugal Compressors and Expander-Compressors", para. 4.9.3.2, Eighth Edition, American Petroleum Institute, Washington, D.C.

Bidaut, Y., Baumann, U., Salim, M. , 2009, "Rotordynamic Stability of a 9500 Psi Reinjection Centrifugal Compressor Equipped with a Hole Pattern Seal – Measurement versus Prediction Taking into Account the Operational Boundary Conditions", Proceedings of the 38th Turbomachinery Symposium, Turbomachinery Laboratory, Texas A&M University College Station, TX.

Bidaut, Y. and Dessibourg, D., 2014, "The Challenge for the Accurate Determination of the Axial Rotor Thrust in Centrifugal Compressors", Proceedings of the 43rd Turbomachinery Symposium, Turbomachinery Laboratory, Texas A&M University College Station, TX.

Da Soghe, R., Facchini, B., Innocenti, L., Micio, M., 2009, "Analysis of Gas Turbine Rotating Cavities by an One-Dimensional Model", Proceedings of ASME Turbo Expo 2009, GT2009-59185.

Gülich, J. F., 2003, "Disk friction losses of closed turbomachine impellers", Forschung im Ingenieurwesen 68, Springer-Verlag, Berlin, Germany.

Halling, J., 1978, "Principles of Tribology", Scholium International, Port Washington, NY.

Kurz, R., Marechale, R., Fowler, E., Ji, M., Cave, M., 2011, "Operation of Centrifugal Compressors in Choke Conditions", Proceedings of the 40th Turbomachinery Symposium, Turbomachinery Laboratory, Texas A&M University College Station, TX.

Lüdtke, K. H., 2004, "Process Centrifugal Compressors", Springer, Berlin, Germany.

Moll, M.D., Postill, J., 2011, "Correction of Chronic Thrust Bearing Failures on a Refrigeration Compressor", Case Study, Proceedings of the 40th Turbomachinery Symposium, Turbomachinery Laboratory, Texas A&M University College Station, TX.

Owen, J.M. and Rogers, R.H., 1989, *Flow and Heat in Rotating Disc Systems*, John Wiley and Sons, NY.

ACKNOWLEDGEMENTS

The authors would like to thank Luisa Ronca and Sara Abbate for their help in the organization of testing activities of compressors equipped with load cells; Valentina Bisio for the technical definitions of load cells provisions and insights on test plan; Davide Vagelli, Gabriele Scotto and Marco Innocenti for their support during test activities.